APPROXIMATE G^1 CUBIC SURFACES FOR DATA APPROXIMATION

Yingbin Liu and Stephen Mann
University of Waterloo, Waterloo, Ontario, Canada

Keywords: CAGD, Triangular Bézier patches, Continuity.

Abstract: This paper presents a piecewise cubic approximation method with approximate G^1 continuity. For a given triangular mesh of points with arbitrary topology, one cubic triangular Bézier patch surface is constructed. The resulting surfaces have G^1 continuity at the vertex points, but only requires approximate G^1 continuity along the macro-patch boundaries so as to lower the patch degree. While our scheme cannot generate the surfaces in as high quality as Loop's sextic scheme, they are of half the polynomial degree, and of far better shape quality than the results of interpolating split domain schemes.

1 INTRODUCTION

In computer graphics applications, a surface is usually constructed from a given data set that represents more or less precisely the surface shape. Due to their elegant geometric properties, triangular Bézier patches are often used to interpolate or approximate a triangulated data mesh. The main difficulty to interpolate or approximate a given data mesh is how to satisfy the restrictions imposed on the control points to obtain surface patches that meet with a given order of continuity. In most cases, we want the surface patches to be visually smooth and meet with G^1 continuity.

In past work, different G^1 schemes using domain splits were devised to fit multiple patches (three or four) to each data triangle (Peters, 1990; Piper, 1987; Shirman and Séquin, 1991; Hahmann and Bonneau, 2003; Mann et al., 1992). Since it is impossible to generated G^1 continuous surfaces on arbitrary data sets using cubic patches (Piper, 1987; Peters, 1990), these schemes use at least quartic patches to guarantee G^1 continuity along the macro-patch boundaries. It was later shown that the results from these local interpolation schemes do not generate satisfactory shapes (Mann et al., 1992). Loop designed a scheme using sextic triangular Bézier patches in one-to-one correspondence with the data triangles (Loop, 1994). In Loop's scheme, an approximation method using transformed data vertices was also presented to create smooth surfaces with high quality. In all these schemes, control points are set to meet the constraints required by G^1 continuity along the patch boundaries. The price to fulfil the G^1 constraints is that we have to use high degree (at least quartic) and/or multiple patches and possibly sacrifice shape quality.

Approximate G^1 continuity is a relaxation of G^1 continuity where patches meet C^0 but the discontinuity in the surface normals between adjacent patches is small. Previous work on approximate G^1 constructions includes parametric interpolation of positions, normals, and second fundamental forms at the data points (Mann, 1992); interpolations with cubic precision on positions and normals at the data points, both in the functional case (Liu and Mann, 2005) and the parametric case (Liu and Mann, 2007). In this paper, the given data network is approximated by integrating techniques from Loop's scheme to construct the boundary curves (Loop, 1994). For each data triangle, three cubic triangular patches are created to meet with C^1 continuity. As for the macro-boundaries, i.e., the boundaries between patches from different data triangles, since we only require approximate G^1 continuity, some discontinuity exists in the surface normals. To decrease this normal discontinuity, two neighbouring patches across the macro-patch boundaries are adjusted later to have equal normals at the middle point

Liu Y. and Mann S. (2008).
APPROXIMATE G1 CUBIC SURFACES FOR DATA APPROXIMATION.
In *Proceedings of the Third International Conference on Computer Graphics Theory and Applications*, pages 39-44
DOI: 10.5220/0001093400390044

on the common boundary curve.

The remaining parts of this paper are arranged as follows: Section 2 reviews the G^1 continuity constraints; the details of our approximation is introduced in Section 3; in Section 4, we show some resulting surfaces, which we compare to surfaces generated by other G^1 schemes; conclusions and possible future work are presented in Section 5.

2 CONTINUITY CONSTRAINTS

A triangular Bézier patch of degree n is defined as

$$S(u,v,w) = \sum_{i+j+k=n} P_{ijk} B^n_{ijk}(u,v,w).$$

Here (u,v,w) are barycentric coordinates for the parameter; $B^n_{ijk}(u,v,w)$ is the generalized Bernstein polynomial; P_{ijk} are the control points of the patch. For two triangular patches to join each other with G^1 continuity, i.e., the tangent planes from the two adjacent patches are coplanar at any point along the boundary curve, certain constraints must be fulfilled.

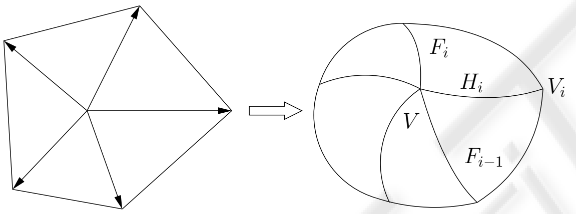

Figure 1: G^1 continuity at a vertex.

For a vertex V with valence n in our mesh, we number the surrounding patches F_i, $i = 0,\dots,n-1$, in anti-clockwise order. Figure 1, right, shows a pair of neighbouring patches F_{i-1} and F_i with common boundary H_i, with their domain triangles appearing on the left of the figure. The parametric direction for the partial derivative along the common edge is defined from V to V_i in the domain triangles.

In this paper, we focus on cubic Bézier patches to explore the G^1 continuity conditions. Two adjacent cubic patches F_i and F_{i-1} with their control points are shown in Figure 2. We define the following vectors:

$$\vec{u}_j = H_i^{j+1} - H_i^j, \quad \vec{v}_j = F_i^j - H_i^j, \quad \vec{w}_j = F_{i-1}^j - H_i^j,$$

with $j = 0,1,2$. Then for any given point along the boundary curve, the tangent planes calculated from the two patches are defined by vectors $\vec{u}$, $\vec{v}$ and $\vec{w}$, all of which are quadratic Bézier functions:

$$\vec{u} = \sum_{j=0}^{2} \vec{u}_j B^n_j(t), \quad \vec{v} = \sum_{j=0}^{2} \vec{v}_j B^n_j(t), \quad \vec{w} = \sum_{j=0}^{2} \vec{w}_j B^n_j(t).$$

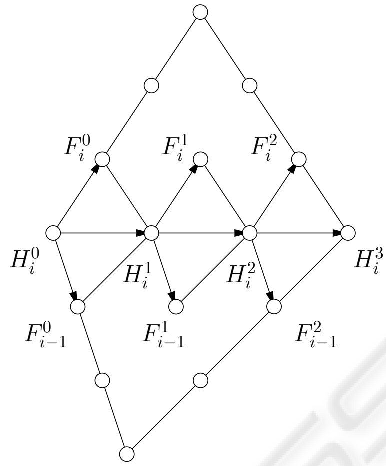

Figure 2: Adjacent cubic patches.

If patches F_i and F_{i-1} meet with G^1 continuity, they must share the control points of the common boundary H_i^j, $j = 0,1,2,3$. Moreover, the two tangent planes at any boundary point should be coplanar, i.e., there exist scalar valued functions $\phi(t)$, $\mu(t)$ and $\nu(t)$ such that for any parameter value t, $t \in [0,1]$, we have

$$\phi(t)\vec{u} = \mu(t)\vec{v} + \nu(t)\vec{w}. \qquad (1)$$

To guarantee the proper orientation of the tangents, assume $\mu(t)\nu(t) \geq 0$. Since it is not guaranteed to create surface using cubic patches to have G^1 continuity (Piper, 1987; Peters, 1990), all the existing G^1 schemes use at least quartic patches (Shirman and Séquin, 1991; Mann et al., 1992)

For all the patches to meet with G^1 continuity at vertex V, the G^1 constraints of Equation 1 are applied to all boundaries originating from vertex V. Differentiating these equations and evaluate at vertex V results in a linear system. Solving this system is called the "twist compatibility" or "vertex consistency" problem, and it has been shown that this linear system may not have a solution (Watkins, 1988; Sarraga, 1988; Loop, 1994). Even if there exists a G^1 solution by solving the twist compatibility problem, it is not clear that the resulting surface has a satisfactory shape.

In the past work, one approach to construct G^1 continuous surfaces is to perform a Clough-Tocher like domain split on each patch F_i surrounding vertex V (Clough and Tocher, 1965). At least quartic degree patches are used in a domain split method (Shirman and Séquin, 1991). Alternatively, Loop invented a solution to solve the twist compatibility using one sextic patch for each data triangle (Loop, 1994), with details introduced in Section 3.1.

Instead of using high degree patches to fulfil the G^1 constraints, we focus on using low degree (cubic) patches to create surfaces with approximate G^1

continuity. With the approximate G^1 method, we allow a small amount of normal discontinuity across the boundary curves. However, we still require G^1 continuity at the vertex points to keep the surface discontinuity going too high. Using the freedom provided by this relaxation, the goals of our method include:

- Use of cubic patches,
- Better shaped surfaces.

3 CUBIC APPROXIMATION

The goal of our work is to approximate the shape represented by a given data mesh as accurately as possible, but using lower degree patches than the G^1 schemes. We achieve this reduction in degree by only requiring approximate G^1 continuity along patch boundaries. In the cubic scheme we describe in this paper, we construct the surface by creating boundary curves for each edge of a data triangle, and then perform a Clough-Tocher like domain split on the cubic patch. After the interior of the patches is filled, we then do some adjustments to lower the normal discontinuity along the boundaries.

3.1 Loop's Scheme

In Loop's scheme, boundary curves are constructed so that the solutions for the twist terms are guaranteed (Loop, 1994). Loop's sextic scheme has the following steps:

1. Construct quartic boundary curves.
2. Solve the twist terms.
3. Construct tangent fields along the boundaries.
4. Elevate the degree of the boundary curves to sextic.
5. Set the second row of control points in the sextic patch to interpolate the tangent fields.
6. Set the remaining center control point by averaging the control points from above steps.

When the valences of the three vertices of a data triangle are equal, the patch constructed by Loop's scheme is quintic; if the three valences are all six, then the patch degree reduces to quartic (Loop, 1994). Our cubic scheme integrated the boundary tangents construction from the first step in Loop's scheme, but generating cubic boundary curves.

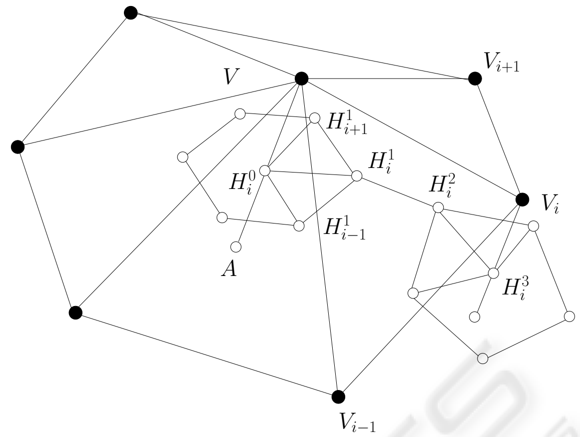

Figure 3: Construction of boundary curves.

3.2 Boundary Construction

For the edge between the vertex V and its neighbour V_i, we use some ideas of Loop (Loop, 1994) to construct a cubic boundary curve H_i, as illustrated in Figure 3. Since the curve is cubic, there are four control points: $H_i^0, H_i^1, H_i^2, H_i^3$ to be constructed. For the vertex V, the control points H_i^0 and H_i^1 are constructed as

$$H_i^0 = \alpha V + (1-\alpha)A = \alpha V + \frac{1-\alpha}{n}\sum_{k=0}^{n-1} V_k, \quad (2)$$

$$H_i^1 = H_i^0 + \frac{\beta}{n}\sum_{k=0}^{n-1}\left[\cos\left(\frac{2(k-i)\pi}{n}\right)\right] V_k. \quad (3)$$

Here n is the valence of the vertex V; point A is the average of all neighbours of vertex V; α and β are two shape parameters. When $\alpha = 1$, the resulting surface interpolates the data vertices, shown as V_i in Figure 3. For α to be other values, the resulting surface approximates the given data mesh. Parameter β defines the length of the tangent vector at H_i^0. In our cubic approximation scheme, the α and β are set with an experimental value the same as in Loop's scheme:

$$\begin{aligned} \alpha &= \frac{1}{9}\left[4+\cos(\frac{2\pi}{n})\right], \\ \beta &= \frac{1}{3}\left[1+\cos(\frac{2\pi}{n})\right]. \end{aligned} \quad (4)$$

With this α value, our scheme does not interpolate the given data vertices, but generating an surface approximating the shape of the given data mesh.

The construction of control points H_i^0 and H_i^1 performs a first order Fourier transformation on all the neighbouring vertices of V (Loop, 1994; Davis, 1979). If all the control points H_i^1 are connected, they form a regular n-gon with H_i^0 being the centre, as shown in the Figure 3. Point H_i^0 is the affine combination of the data vertex V and the average center of V's neighbours, and all the boundary curves connecting V share the same position of point H_i^0. The other two control points H_i^2 and H_i^3 are calculated similarly with Equation 3, using the information of V_i's neighbours.

In Loop's scheme, quartic boundary curves have to be used to fulfil the strict G^1 continuity conditions, and later the patch degree is elevated to sextic for the same reason.

3.3 Patch Construction

Past work shows that it can be impossible to generate G^1 continuous surfaces using cubic patches (Piper, 1987; Peters, 1990). When using approximate G^1 continuity, we found there was insufficient degrees of freedom if we only used one cubic patch per data triangle. In particular, with one cubic patch per face, since the center control point of this patch affects the normals along all three boundaries, it is difficulty to place this control point to yield surfaces with acceptable smoothness. To improve surface smoothness and still use cubics, we perform a Clough-Tocher like domain split (Clough and Tocher, 1965) to construct three micro-patches for each data triangle.

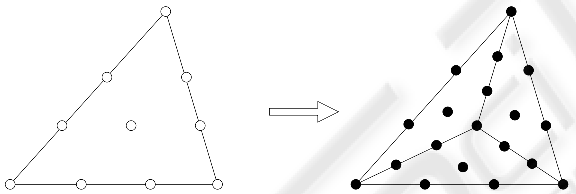

Figure 4: Macro patch split.

We first construct one cubic patch for each data triangle, as shown on the left in Figure 4. The boundaries of this initial patch are set with the methods described in Section 3.2. We set the center control point to be the weighted average of the other nine control points, using a method similar to the way introduced in one author's previous paper (Mann, 1999).

We then subdivide the patch into three cubic patches (called micro patches), as shown in the right of Figure 4. The subdivided control points are shown as small black dots in Figure 5. The small white and the big white points are constructed as the gravity centre of the adjacent three control points, as in Clough-Tocher's scheme (Clough and Tocher, 1965; Farin, 1986; Mann, 1999). After the split, the center control point of each micro-patch, shown as big black dots in Figure 5, only affects the continuity along the corresponding macro-patch boundary. The initial positions

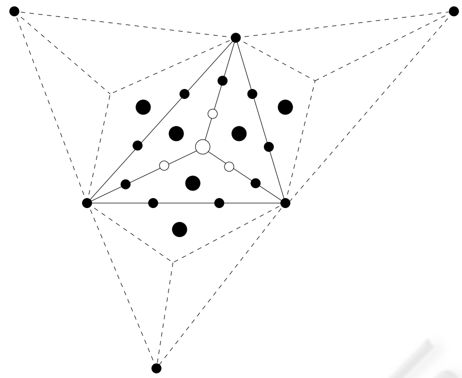

Figure 5: Control points construction.

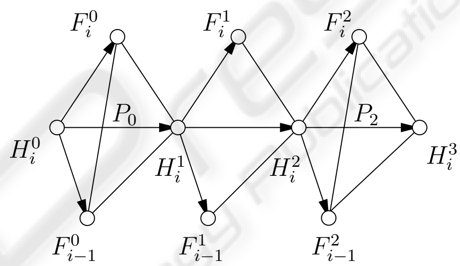

Figure 6: Ratios of intersection.

for these three points are set by local averaging. As shown in Figure 6, The two pairs of side panels are set to be coplanar to have equal normals at end data points H_i^0 and H_i^3. Let $F_i^0F_{i-1}^0$ intersect $H_i^0H_i^1$ at P_0, $F_i^2F_{i-1}^2$ intersect $H_i^2H_i^3$ at P_2, as shown in Figure 6. Here the points F_i^j and F_{i-1}^j $(j = 0,1,2)$ are the micro patch control points resulting from the Clough-Tocher like split. The ratios of the intersection are then defined as

$$\eta_0 = \frac{|P_0 - H_i^0|}{|H_i^1 - H_i^0|}, \qquad \gamma_0 = \frac{|F_{i-1}^0 - P_0|}{|F_{i-1}^0 - F_i^0|},$$
$$\eta_2 = \frac{|P_2 - H_i^2|}{|H_i^3 - H_i^2|}, \qquad \gamma_2 = \frac{|F_{i-1}^2 - P_2|}{|F_{i-1}^2 - F_i^2|}.$$

We set the initial position for point F_i^1 and F_{i-1}^1 as

$$\begin{aligned} F_i^1 &= H_i^1 + \left(1 - \frac{\gamma_0+\gamma_2}{2}\right)\frac{F_i^0 - F_{i-1}^0 + F_i^2 - F_{i-1}^2}{2} \\ &\quad + \frac{\eta_0+\eta_2}{2}(H_i^2 - H_i^1), \\ F_{i-1}^1 &= H_i^1 - \frac{\gamma_0+\gamma_2}{2}\,\frac{F_i^0 - F_{i-1}^0 + F_i^2 - F_{i-1}^2}{2} \\ &\quad + \frac{\eta_0+\eta_2}{2}(H_i^2 - H_i^1). \end{aligned} \tag{5}$$

The two center control points across the macro-patch boundary are then adjusted by adding an offset vector that is calculated with the method introduced in our previous paper. After the adjustments, the normal vectors of two patches at the middle boundary point is equal. Theoretically, we can adjust the center points to have equal normals at two or three points along the boundary, but that will make the scheme not stable. In all the examples shown in Section 4, all the surfaces by our scheme have equal normals only at one middle boundary points.

This cubic scheme is approximately G^1 along the macro-patch boundaries, although patches meet with G^1 continuity at the vertex points; the patches meet with C^1 continuity along the boundaries between two micro-patches; and the three micro-patches meet with C^2 at the split point, a result of the averaging in Step 3 of (Farin, 1986).

4 RESULTS

We compared the resulting surfaces of our cubic scheme to those generated by Loop's scheme, with both the interpolation and the approximation results. Since Loop's scheme does not use the domain split method, we also generated surfaces on the same models using Shirman-Séquin's quartic scheme to make the comparison more comprehensive. Shirman-Séquin's scheme generates surfaces with data vertices interpolated, and it also performs a domain split similar to Clough-Tocher's (Shirman and Séquin, 1991).

In Figure 7, we show four surfaces fit to an icosahedron. The top left is Loop's interpolating surface; the bottom left is Loop's approximating surface; the top right is the quartic, G^1 scheme by Shirman-Séquin; the bottom right is our cubic, approximate G^1 scheme. Loop's approximate scheme has much better shape than his interpolating scheme; our cubic approximation scheme has similar shape to Loop's. The highest normal discontinuity is 0.48 degree on our cubic surface.

In Figure 8, we show four surfaces fitted to the Stanford bunny model. The order of the schemes is the same as in Figure 7. While the two interpolating schemes show numerous shape artifacts, both approximating schemes produce surfaces with far better shape quality. In this model, the highest normal discontinuity is 19.57 degree for our cubic surface. However, boundaries with high normal discontinuity angles (more than 10 degrees) account for about 0.8% of all boundary curves. While some artifacts are visible in our approximate G^1 scheme, we see substantial improvement over the similar interpolating scheme.

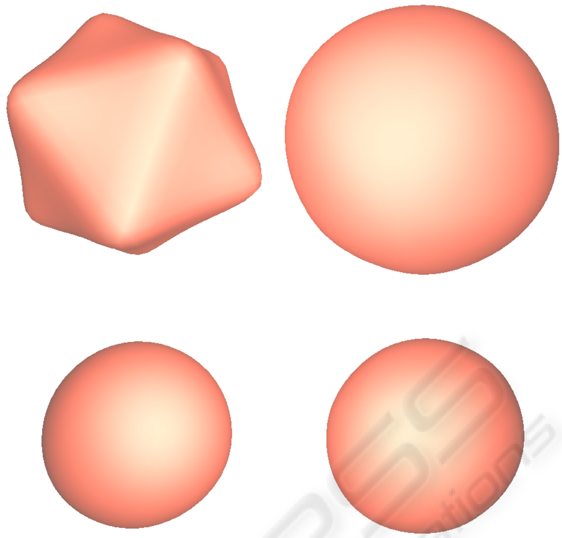

Figure 7: Icosahedron surfaces.

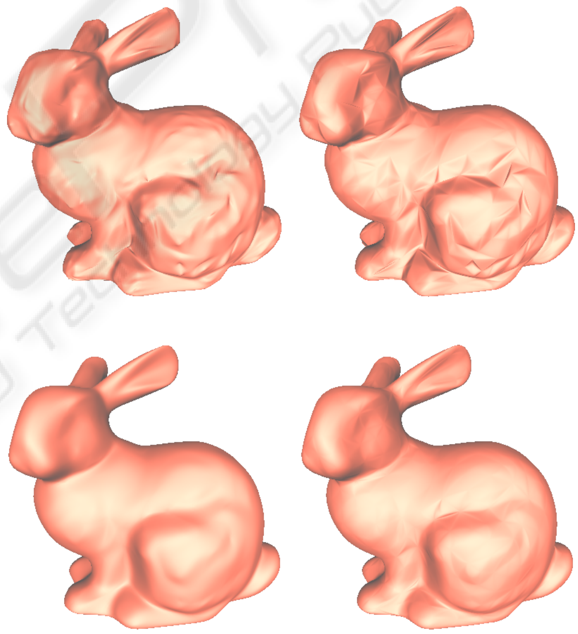

Figure 8: Bunny surfaces.

5 CONCLUSIONS

In this paper we presented a cubic approximating scheme to generate surfaces characterizing the shape of given data mesh with low price. Although the normal discontinuities on the resulting surfaces are visible on some test models, the overall surface shape is good. Further, our scheme is only cubic and it will offer great advantage for easy implementation and stability.

In the future, we will do further analysis on the cross boundary discontinuity, and derive an upper bound for it. We will also look for methods to guarantee that the normal discontinuity does not exceed a specified bound. This will likely result in conditions similar to the vertex consistency conditions, but our expectation is that we will be able to trade patch shape for lower normal discontinuity.

REFERENCES

Clough, R. and Tocher, J. (1965). Finite element stiffness matrices for analysis of plates in bending. In *Proceedings of Conference on Matrix Methods in Structural Analysis*.

Davis, P. (1979). *Circulant Matrices*. Wiley, New York.

Farin, G. (1986). Triangular Berstein-Bézier patches. *Computer Aided Geometric Design*, 3(2):83–127.

Hahmann, S. and Bonneau, G.-P. (2003). Polynomial surfaces interpolating arbitrary triangulations. *IEEE Transactions on Visualization and Computer Graphics (TVCG)*, 9(1):99–109.

Liu, Y. and Mann, S. (2005). Approximate continuity for functional, triangular Bézier patches. *SIAM-Geometric Modeling 2005*.

Liu, Y. and Mann, S. (2007). Approximate continuity for parametric bézier patches. *ACM Solid and Physical Modeling Symposium*.

Loop, C. (1994). A G^1 triangular spline surface of arbitrary topological type. *Computer Aided Geometric Design*, 11(3):303–330.

Mann, S. (1992). *Surface Approximation Using Geometric Hermite Patches*. PhD thesis, University of Washington.

Mann, S. (1999). Cubic precision clough-tocher interpolation. *Computer Aided Geometric Design*, 16(2):85–88.

Mann, S., Lounsbery, M., Loop, C., Meyers, D., Painter, J., DeRose, T., and Sloan, K. (1992). *Curve and Surface Design, Chapter 8, A Survey of Parametric Scattered Data Fitting Using Triangular Interpolants*. SIAM.

Peters, J. (1990). Smooth mesh interpolation with cubic patches. *Computer-aided Design*, 22/2:109–120.

Piper, B. P. (1987). Visually smooth interpolation with triangular bézier patches. In Farin, G., editor, *Geometric Modeling: Algorithms and New Trends*, pages 221–234. SIAM.

Sarraga, R. F. (1988). G^1 interpolation of generally unrestricted cubic bézier curves. *Computer Aided Geometric Design*, 4(1-2):23–40.

Shirman, L. and Séquin, C. (1991). Local surface interpolation with bézier patches: Errata and improvements. *Computer Aided Geometric Design*, 8(3):217–221.

Watkins, M. A. (1988). Problems in geometric continuity. *Computer Aided Geometric Design*, 20(8):499–502.